Journal of
Materials Chemistry B

PAPER

View Article Online
View Journal

Cite this: DOI: 10.1039/c7tb03239k

A 3D *in vitro* pericyte-supported microvessel model: visualisation and quantitative characterisation of multistep angiogenesis†

Eujin Lee,[a] Haruko Takahashi,[a] Joris Pauty,[ab] Masayoshi Kobayashi,[c] Keisuke Kato,[c] Maki Kabara,[d] Jun-ichi Kawabe[d] and Yukiko T. Matsunaga *[ab]

Angiogenesis, which refers to the formation of new blood vessels from already existing vessels, is a promising therapeutic target and a complex multistep process involving many different factors. Pericytes (PCs) are attracting attention as they are considered to make significant contributions to the maturation and stabilisation of newly formed vessels, although not much is known about the precise mechanisms involved. Since there is no single specific marker for pericytes, *in vivo* models may complicate PC identification and the study of PCs in angiogenesis would benefit from *in vitro* models recapitulating the interactions between PCs and endothelial cells (ECs) in a three-dimensional (3D) configuration. In this study, a 3D *in vitro* co-culture microvessel model incorporating ECs and PCs was constructed by bottom-up tissue engineering. Angiogenesis was induced in the manner of sprout formation by the addition of a vascular endothelial cell growth factor. It was found that the incorporation of PCs prevented expansion of the parent vessel diameter and enhanced sprout formation and elongation. Physical interactions between ECs and PCs were visualised by immunostaining and it disclosed that PCs covered the EC monolayer from its basal side in the parent vessel as well as angiogenic sprouts. Furthermore, the microvessels were visualized in 3D by using a non-invasive optical coherence tomography (OCT) imaging system and sprout features were quantitatively assessed. It revealed that the sprouts in EC–PC co-culture vessels were longer and tighter than those in EC mono-culture vessels. The combination of the microvessel model and the OCT system analysis can be useful for the visualisation and demonstration of the multistep process of angiogenesis, which incorporates PCs.

Received 15th December 2017,
Accepted 15th January 2018

DOI: 10.1039/c7tb03239k

rsc.li/materials-b

1 Introduction

Angiogenesis, which refers to the formation of new blood vessels from already existing vessels, is a promising therapeutic target as its suppression can lead to tumour regression, whereas its promotion can result in regeneration of the tissue environment in ischaemic cardiovascular diseases such as stroke. Microvessels consist of a cylindrical tube of endothelial cell (EC) layers surrounded by pericytes (PCs), which mechanically support the microvessels. Angiogenesis is a multistep process that starts with ECs losing contact inhibition and degradation of the basement membrane, followed by the migration of specialised ECs called tip cells towards an angiogenic stimulus, such as vascular endothelial growth factor (VEGF).[1] Endothelial stalk cells then proliferate to elongate the newly formed vessel and the new basement membrane is created. This process is further complemented by an association with PCs.[2]

Within the context of angiogenesis, PCs are considered to exert diverse functions including modulation of the extracellular matrix, paracrine signalling and adjustment of the local mechanical environment by contraction, and are in some cases thought to lead to sprout formation by migrating prior to ECs and secreting growth factors.[3,4] Based on previous discussions,[5,6] PCs are recruited to the site of angiogenesis after the sprouting of ECs, and the absence of PCs is considered to liberate ECs to remodel, proliferate or regress depending on the absence or presence of growth factors. Hence, PCs not only assist new sprout formation but are also thought to cause growth arrest in ECs and stabilise vessels.

[a] Center for International Research on Integrative Biomedical Systems (CIBiS), Institute of Industrial Science, The University of Tokyo, 4-6-1 Komaba, Meguro-ku, Tokyo 153-8505, Japan. E-mail: mat@iis.u-tokyo.ac.jp; Fax: +81-3-5452-6471; Tel: +81-3-5452-6470
[b] LIMMS/CNRS-IIS (UMI 2820), Institute of Industrial Science, The University of Tokyo, 4-6-1 Komaba, Meguro-ku, Tokyo 153-8505, Japan
[c] R&D Department 1, SCREEN Holdings Co., Ltd, 322 Furukawa-cho, Hazukashi, Fushimi-ku, Kyoto 612-8486, Japan
[d] Department of Cardiovascular Regeneration and Innovation, Asahikawa Medical University, Midorigaoka, Higashi 2-1-1, Asahikawa, Hokkaido 078-8510, Japan

† Electronic supplementary information (ESI) available. See DOI: 10.1039/c7tb03239k

EC and PC interactions are thought to be mediated by angiopoietin-1 (ANG-1) and TIE-2 receptor signalling, in which PC derived ANG-1 binds to TIE-2 receptors on ECs and cause vessel maturation and stabilization.[7–9] Although PCs are known to be essential for angiogenesis, the exact mechanism by which they control EC dynamics remains poorly understood, partly because there is no single specific marker that can identify PCs. Hence, PCs are commonly identified by the co-expression of several markers, such as platelet-derived growth factor-β receptor (PDGFR-β), neural/glial antigen 2 (NG2) and α-smooth muscle actin (α-SMA). However, PC marker expression varies among different tissues and at different developmental stages, presenting an obstacle for identification.[7]

Established methods for studying *in vivo* angiogenesis include the Matrigel plug assay,[10,11] in which Matrigel containing pro- or anti-angiogenic factors are injected subcutaneously into animals and then removed after a few days for the observation of newly formed vessels in the Matrigel region. The benefits of using this approach include the fact that the degree of angiogenesis can be quantified by the amount of haemoglobin in the gel; however, drawbacks also exist, such as the analysis being time-consuming. Another example of an *in vivo* assay is the corneal angiogenesis assay,[12] in which a pocket is created in the cornea, into which pro- or anti-angiogenic factors are placed. In this model, newly formed vessels can be easily seen as the cornea does not originally possess vasculature and, since the eyes are exposed to the exterior, their removal is not required for observation. Nevertheless, *in vivo* studies involve multiple cell types, making it difficult to study the interactions between ECs and a specific factor. In addition, they require animal handling; the analysis is difficult in many cases and may be time-consuming.[11,13,14] Therefore, an *in vitro* system which enables simplification of the complex *in vivo* system is needed.

In recent years, new bottom-up tissue engineering approaches enabled controlling the spatial arrangement of the cells and tissue structure.[15–20] These *in vitro* techniques as well as others such as a tube formation assay, a cell bead assay, and a microfluidic platform made it possible to visualize how each constituent affects others and further explore the role of PCs in angiogenesis. A tube formation assay, in which ECs and PCs are seeded onto the matrix together to form tube-like structures, demonstrated that PCs interacted with ECs in close proximity, extended EC survival and increased the number and the length of EC tubes formed in an angiogenic setting.[21,22] However, the tube formation assay performs only the remodelling step of angiogenesis, which involves the assembly of ECs into tubes, and does not allow reproduction of the whole process of angiogenesis. Moreover, as this assay relies on the unorganised spontaneous formation of blood vessels in the gel, there is a large variation in the diameter of the tubes formed, which may not be favourable for addressing the contribution of PCs since their presence affects the diameter of the vessels.[23] With the emergence of microfluidic techniques, it has become possible to control the growth direction of sprouts composed of ECs and PCs and to analyse their widths and numbers, as previously reported.[15] By fabricating a device that allows the introduction of ECs and PCs together into the same channel and the co-culture of fibroblasts in distance, angiogenesis can be induced in the direction of fibroblasts as fibroblasts secrete growth factors. In a previous study, it was found that co-culturing ECs with PCs under angiogenic conditions led to the accumulation of basement membrane constituents such as collagen type IV and laminin in the sprouts, whose presence indicates maturation of the formed sprout. It was also discovered that the incorporation of PCs led to an increase in the number of branches and a decrease in the width of the sprouts. Moreover, using a cell bead assay, in which microcarrier beads covered with ECs and PCs form sprouts in all directions in response to angiogenic stimulation, it was found that the incorporation of PCs stabilised formed sprouts as sprouts with EC and PC co-culture were more resistant to compounds thought to modulate angiogenesis, such as inhibitors of vascular endothelial growth factor receptor-2 (VEGFR-2) and PDGFR.[24,25] Using this assay, it was also possible to quantify PC coverage in sprouts by identifying ECs and PCs by nuclear staining. Nevertheless, in these methods, only sprout formation was focused on and sprouts were not generated from pre-existing parent vessels; moreover, it remains unexplored how PCs behave in the parent vessel, therefore their role in the initiation of the angiogenic process remains unclear.

Previously, we proposed a VEGF-induced angiogenesis model, which allows visualisation of the whole angiogenic process, from the first appearance of the sprouts out of the pre-existing vessel to the maturation of the newly formed sprouts.[26,27] This model can demonstrate the angiogenic process from its start, since functional, perfusable and three-dimensional (3D) blood vessels that act as the pre-existing vessels are prepared by applying bottom-up tissue engineering. These equipped blood vessels respond to VEGF by causing dynamic changes in the parent vessel and the development of new vessels in the form of sprouts. However, this model incorporated only ECs and responded mostly to VEGF by expansion or deformation of the parent vessel, rather than elongation of the newly formed sprouts, making it difficult to differentiate VEGF-induced angiogenesis from that without stimulation and to quantify angiogenesis.

To overcome these drawbacks encountered in other *in vitro* studies and our previous angiogenesis model, we aimed to construct a blood vessel model that incorporates both ECs and PCs, hence recreating a more physiological environment. The novelty of our model is that it demonstrated the appearance of sprouts from the pre-existing parent vessel, making it more functional as an angiogenesis model. In addition, it is a simpler *in vitro* model as it does not involve fibroblasts, which are often added to the external space around ECs to induce sprouting in the controlled direction. Furthermore, since ECs and PCs are mixed together during vessel construction and are located close to each other, physical interactions between them can be observed. In this study, we found that the incorporation of PCs into ECs led to the formation of longer and tighter sprouts in response to VEGF, which is more favourable for the quantitative analysis of angiogenesis, and less expansion of the parent vessel was observed as the PCs were providing mechanical support by attaching to the endothelial layer from the outside in sprouts as well as the parent vessel.

2 Materials and methods

2.1 Materials

Type I-A Cellmatrix® collagen derived from porcine tendons by acid extraction (3 mg mL^{-1}, pH 3) was obtained from Nitta Gelatin Inc. (Osaka, Japan). Acupuncture needles (200 μm diameter: J type, No. 3, 30 mm length) were purchased from Seirin Co. Ltd (Shizuoka, Japan). Fibronectin solution (1 mg mL^{-1}) was purchased from Biomedical Technologies Inc. (Stoughton, MA, USA). Hoechst 33342 and Alexa Fluor® phalloidin 568 were purchased from Thermo Fisher Scientific, Inc. (Waltham, MA, USA). Human vascular endothelial growth factor (VEGF-A165) recombinant, 0.5 w/v% trypsin–5.3 mmol L^{-1} EDTA-4Na solution, and 10× phosphate buffer saline (–) (PBS) were purchased from Wako Pure Chemical Industries, Ltd (Osaka, Japan). Dextran from *Leuconostoc* spp. (M_r 450 000–650 000) and Hanks' Balanced Salt Solution (HBSS) were purchased from Sigma-Aldrich Co. LLC. (St. Louis, MO, USA). Mouse anti-human CD31 antibody (0.5 mg mL^{-1}) was purchased from Dako.

2.2 Cell culture

Endothelial cells. Human umbilical vein endothelial cells (HUVECs) and cell culture medium EGM™-2 Endothelial Cell Growth Medium-2 BulletKit™ were purchased from Lonza Japan Ltd (Tokyo, Japan). HUVECs were seeded on tissue culture polystyrene dishes (TCPS) and incubated at 37 °C with 5% CO_2. Once cells reached confluency, they were harvested after 3 min incubation with trypsin–EDTA 0.25% and collected by centrifugation (400 × *g*, 3 min) prior to resuspension in the medium. HUVECs at passage number 4–6 were used to prepare the microvasculature model.

Pericytes. Mouse immortalized capillary-derived PCs were obtained as described previously.[28] PCs were maintained in Dulbecco's Modified Eagle's medium (DMEM) containing 10% FBS at 33 °C. To trace the PCs within the 3D *in vitro* models, cells labeled with fluorescent protein were prepared. Briefly, cells were infected with a recombinant retrovirus harbouring a green fluorescent protein (GFP) gene and a late SV40 polyadenylation signal under the control of the Cytomegalovirus (CMV) promoter. After several passages, the cells expressing GFP stably were sorted using fluorescence-activated cell sorting (FACS) flow cytometry (FACSAria II, Beckman Coulter, Brea, CA).

2.3 Microvessel preparation

Polydimethylsiloxane (PDMS)-based microdevices were prepared as previously reported.[26] The central channels of the PDMS device were covered with a top glass (6.0 × 20.5 mm: width × length) and inner surfaces of the channel were coated with fibronectin (10 μg mL^{-1}) in PBS. Acupuncture needles with a diameter of 200 μm were immersed in 1% (w/w) bovine serum albumin (BSA) in PBS and then introduced through the holes into the channel. The neutralized collagen solution (final concentration of 2.4 mg mL^{-1}) was added to the channels and the devices were incubated at 37 °C for 30 min for solidification of the collagen. Micro-needles were then removed from the collagen to create a hollow space to which cells attach and form a vessel-like structure. A 4 μL aliquot of either HUVECs' suspension [1.0 × 10^7 cells per mL in EGM-2 containing 3% (w/w) dextran] or 4.8 μL of HUVEC and mouse PC (mPC) mixture suspension (1.0 × 10^7 cells per mL in total, mixed in HUVEC : mPC = 5 : 1) was loaded into the collagen gel channels for the preparation of HUVEC mono-culture vessels and HUVEC and mPC co-culture microvessels. Cell suspension volumes were adjusted to make HUVEC with a density of 1.0 × 10^7 cells per mL. Devices were then incubated for 15 min at 37 °C to allow their attachment to the wall of the collagen gel channel. Subsequently, 1.5 mL of EGM-2 was added to cover the collagen gels, and cells were incubated at 37 °C and 5% CO_2 for 2 days. All experiments were performed under the static conditions.

2.4 Angiogenesis induced by VEGF

After 2 days of pre-culture with EGM-2, the medium was changed to EGM-2 containing VEGF at the final concentration of 50 ng mL^{-1}.[26,29] Devices were then incubated at 37 °C and 5% CO_2 for maximum of 8 days. The medium containing VEGF was changed every 48 h. Morphological changes in the microvessels were monitored under a phase contrast microscope with lenses of 10× magnification (Axio Observer D1; Carl Zeiss, Oberkochen, Germany).

2.5 Immunofluorescence staining

Cells were visualized using immunofluorescence staining. After washing with PBS, microvessels were fixed with 4% (w/w) paraformaldehyde (PFA) in PBS for 30 min and then permeabilized with 0.5% Triton-X in PBS for 10 min. Blocking was performed using 1% (w/w) BSA in PBS overnight at 4 °C. For staining CD31, cells were incubated with mouse anti-human CD31 antibody (1 : 200 in PBS) overnight at 4 °C after blocking and then washed with PBS. Cells were then incubated with anti-mouse secondary antibody, Alexa 488 (1 : 200 in PBS) at 25 °C for 4 h. For staining F-actin, cells were exposed to Alexa Fluor 568-phalloidin at 25 °C for 4 h, and for the nucleus, Hoechst 33342 at 25 °C for 15 min after blocking. Microvessels were washed thoroughly with PBS prior to observation.

2.6 Microscopy

Phase-contrast images of the non-stained 3D microvessels were obtained using an Axio Observer Z1 microscope (Axio Observer.Z1; Carl Zeiss, Oberkochen, Germany) with the lens of 10× magnification. Images were processed using software Axiovision Rel. 4.8 (Carl Zeiss). Fluorescent images of the stained 3D microvessels were obtained using a confocal laser scanning microscope (CLSM) (LSM700; Carl Zeiss) with lenses of 10×, 20×, and 40× magnification and a fluorescence microscope (BZ-X700; Keyence, Osaka, Japan) with lenses of 10× magnification. CLSM images were processed using software ZEN version 8.1 (Carl Zeiss) to construct 3D projection images from the Z-stack images.

Parent vessel diameter. Microvessels were cut in half across the center in the images. Three random locations were selected along the parent vessel and the diameter at each location was measured using Axiovision ver. 4.8 (Carl Zeiss). The vessel diameter was obtained by averaging the three measurements.

Since the samples needed to be fixed with PFA for the image analysis with immunostaining, the number of samples decreased as the culture time progressed (EC mono-culture vessels cultured with additional VEGF: 0 day and 3 days, $n = 12$; 5 days, $n = 9$; 8 days, $n = 6$. EC–PC co-culture vessels cultured with additional VEGF: 0 day and 3 days, $n = 8$; 5 days, $n = 6$; 8 days, $n = 3$. EC mono-culture vessels cultured without VEGF: all time points, $n = 3$. EC–PC co-culture vessels cultured without VEGF: all time points, $n = 5$).

Sprout number and length. Sprout lengths were measured from the *X*–*Y* plane images obtained by cutting across the center of the immuno-stained microvessel using CLSM. Sprouts with length greater than 40 μm were counted and measured. (For sprout number, "*n*" represents the number of microvessels, and EC mono-culture vessels cultured with additional VEGF: 3 days, $n = 7$; 5 days and 8 days, $n = 6$. EC–PC co-culture vessels: 3 days, $n = 5$; 5 days, $n = 7$; 8 days, $n = 5$. For sprout length, "*n*" represents the number of sprouts, and EC mono-culture vessels cultured with additional VEGF: 3 days; $n = 31$, 5 days, $n = 43$; 8 days, $n = 56$. EC–PC co-culture vessels: 3 days, $n = 50$; 5 days, $n = 97$; 8 days, $n = 88$.)

2.7 3D optical coherence tomography (OCT) observation

An OCT setup was developed as previously described,[26] but with some modifications to increase the optical resolution to 3 μm: the voxel size was 2 μm × 2 μm × 2 μm and the beam diameter was 10 μm. The average data acquisition window was 700 μm × 700 μm × 700 μm (height × width × length) which correlates with 351 scans per axis observed in 30 min. For 3D images, original cross-sectional images captured using the OCT system were processed using ImageJ (National Institute of Health, USA) to reduce the noise arising from the collagen gel, by subsequently applying the following filters: (i) 3D maximum, (ii) 3D Gaussian low-pass, (iii) 2D FFT band-pass, and (iv) 3D Gaussian low-pass. Then 3D images were constructed using the ImageJ plugin: 3D viewer.

In order to quantitatively assess the features of the angiogenic sprouts, the following method was applied in ImageJ processing: (i) the gray image of a sprout was converted into a 3D binary image; (ii) volume and surface were calculated using the 3D Objects Counter function; (iii) 3D binary image of the sprout was skeletonized using the plugin Skeletonize (2D/3D); (iv) the length of sprout was measured using the Analyze Skeleton (2D/3D); and (v) finally, the average diameter of the sprout was calculated from its volume and length based on the assumption that its cross section is circular. For the quantification, $n = 10$ sprouts for EC mono-culture and $n = 36$ sprouts for EC–PC co-culture.

3 Results

3.1 Preparation of the 3D EC–PC co-culture angiogenesis microvessel model

We aimed to develop a stable 3D microvessel model composed of ECs and PCs. Angiogenesis is a multistep process that involves both ECs and PCs, although it is still under debate how the PCs act in the context of angiogenesis. It is proposed that angiogenesis begins with PC detachment from the EC layer, and PC migration prior to EC migration leads to the sprouting process.[30,31] ECs lose contact inhibition and migrate towards an angiogenic stimulus as tip cells, which is followed by EC proliferation to form sprouts and coverage of the newly formed sprouts by PCs for stabilisation, as shown in Fig. 1a. To develop a 3D microvessel model incorporating both ECs and PCs, which allows demonstration of the angiogenic process from the appearance of sprouts from the pre-existing vessel, we used a PDMS device with three dumbbell-shaped chambers, as shown in Fig. 1b. To establish the EC–PC co-culture system, ECs and PCs were mixed first and were introduced together into the hollow space (200 μm in diameter) in the collagen after the removal of the needle, as shown in Fig. 1c. Microvessels were then cultured with EGM-2 to allow cells to attach firmly to the collagen and adhere to each other to form a vessel-like morphology. Having confirmed that the EC–PC co-culture vessels were stable after the 2 day pre-culture period, they were then cultured with additional VEGF in EGM-2. Previously we tested a range of VEGF concentrations and established a highly reproducible long-term response in EC mono-culture vessels at 50 ng mL^{-1}, which is considered as the concentration that is sufficiently high to induce angiogenesis in the manner of sprout formation in other *in vitro* studies.[26,32] This VEGF concentration was also found to successfully induce sprout formation in EC–PC co-culture vessels in the same manner.

We examined a range of EC : PC ratios (4 : 1, 5 : 1 and 10 : 1) to determine the optimum for the VEGF-induced angiogenesis model, in terms of ensuring sufficient stability of the microvessels so that they do not collapse after the addition of VEGF (50 ng mL^{-1}) (Fig. S1, ESI†). When ECs and PCs were mixed at a 10 : 1 ratio, there was no visible difference between EC mono-culture and EC–PC co-culture in terms of parent vessel or sprout characteristics, even after the addition of VEGF. When the EC : PC ratio was less than 4 : 1, microvessels started to tear apart due to vigorous PC migration in the early period, not allowing the formation of a continuous layer. The optimum EC : PC ratio in this model was 5 : 1, with which the continuous layer was maintained and distinguishable sprout formation was observed in response to VEGF addition.

3.2 VEGF-induced angiogenesis in the EC–PC co-culture vessel

We investigated angiogenic responses in EC–PC co-culture vessels and compared them with those observed in EC mono-culture vessels. To check whether the presence of PCs alone can induce any visible angiogenic changes in the EC layer, we cultured EC–PC co-culture vessels and EC mono-culture vessels as a control without VEGF stimulation for 5 days, and observed the morphological changes using a bright-field microscope (BFM) (Fig. 2a). When EC mono-culture vessels were cultured without additional VEGF, no visible changes were observed over time, with vessels maintaining the tube structure as was seen at day 0. Meanwhile, in EC–PC co-culture vessels, some cells migrated into the collagen gel during the first 2 days which

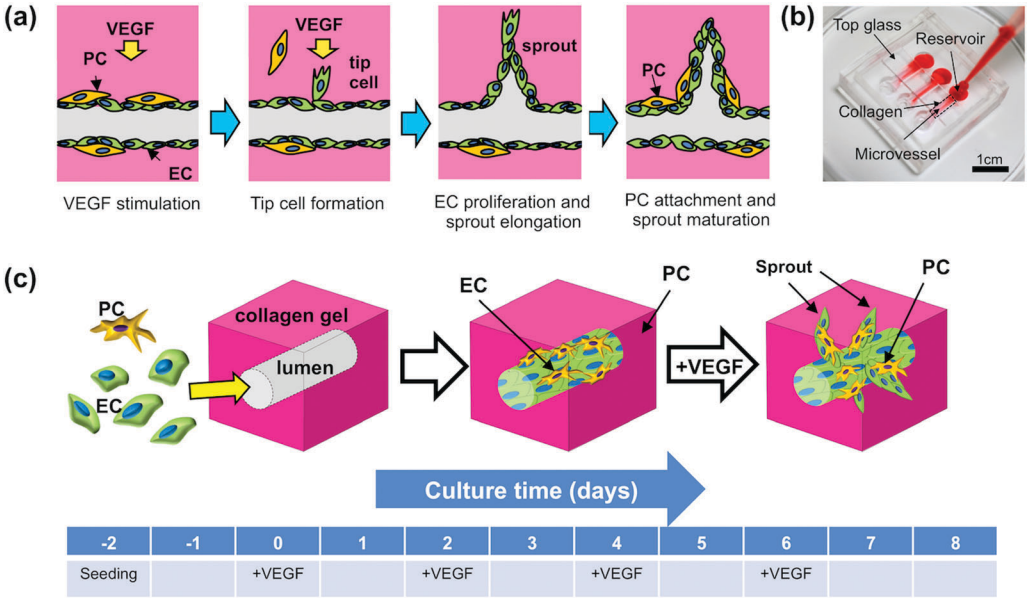

Fig. 1 A schematic view of angiogenesis highlighting endothelial cell (EC) and pericyte (PC) involvement and the method used to create the EC–PC co-culture system. (a) Steps of angiogenesis: first, VEGF stimulation causes detachment of PCs and ECs lose contact inhibition. Next, specialised types of ECs called tip cells migrate towards VEGF, followed by EC proliferation and elongation of the newly formed spouts. Finally, sprouts are covered with PCs for stabilisation. (b) Microfluidic PDMS device with three dumbbell-shaped chambers used to construct the microvessel model. The centre parts of the dumbbell-shaped chambers contain collagen gel and are covered with a top glass. Microvessels are present in the collagen and the lumen is filled with the red ink flowing in from the reservoirs. (c) The process of microvessel construction and culture regimen: ECs and PCs were mixed together and introduced into the hollow space created in the collagen after the removal of a needle. Cells were cultured with EGM-2 for 2 days and then with EGM-2 with additional VEGF for a maximum of 8 days.

corresponds to the pre-culture period, which was never seen in EC mono-culture vessels. Nevertheless, EC–PC co-culture vessels neither developed sprouts nor showed any significant changes in the parent vessel throughout the culture period without additional VEGF, which was similar to the findings observed in EC mono-culture vessels. Hence, PCs alone were incapable of inducing significant morphological changes in this model without the stimulation by VEGF. Meanwhile, when VEGF (50 ng mL^{-1}) was added to the microvessels, sprouts started to emerge in both EC mono-culture and EC–PC co-culture vessels after three days, but the extent to which sprouts elongated over time differed, as shown in Fig. 2a. Sprouts continuously extended in EC–PC co-culture vessels, whereas those in EC mono-culture vessels remained similar in length. With respect to the parent vessel, the diameter continuously increased in EC mono-culture vessels, whereas that in EC–PC co-culture vessels remained similar.

Fig. 2b shows the quantified changes in the average parent vessel diameter over time in EC mono-culture and EC–PC co-culture when cultured with or without additional VEGF. When cultured without additional VEGF, EC vessels presented no significant changes in the diameter, maintaining the same size as was exhibited before the addition of VEGF, which was 194.7 ± 14.2 μm. Similarly, in EC–PC co-culture vessels, although there was a slight decrease in EC–PC co-culture vessels over time from 208.7 ± 6.8 to 172.5 ± 7.9 μm by 5 days, when cultured with additional VEGF, the average parent vessel diameter for EC mono-culture was 201.9 ± 6.9 μm at 0 day and continuously increased to reach 319.1 ± 28.5 μm at day 8, which was almost 1.5 times greater than that at 0 day. Meanwhile, the average parent vessel diameter of EC–PC co-culture increased from 193.3 ± 10.4 at day 0 to 237.6 ± 12.4 μm at day 3 and then maintained the same diameter up to 8 days. Changes in the sprout length and number are quantified in Fig. 2c and d, respectively. On the one hand, the number of sprouts increased notably over time in EC–PC co-culture, from 3.3 ± 0.8 sprouts at day 3 to 5.9 ± 0.9 sprouts per 1 mm parent vessel at day 8 (Fig. 2c); similarly, the length increased from 106.8 ± 6.6 μm at day 3 to 198.4 ± 10.9 μm at day 8 (Fig. 2d). On the other hand, in EC mono-culture vessels, the number of sprouts remained similar at around two sprouts per 1 mm parent vessel from day 3 to day 8 and even showed a slight decrease at day 8, and the sprout length was also maintained at around 70 μm from day 3 to day 8.

Taking these findings together, upon developing a 3D EC–PC co-culture angiogenesis model and comparing the responses to VEGF to those in EC mono-culture vessels, we found that the incorporation of PCs prevents expansion of the parent vessel diameter, and enhances sprout formation and elongation.

3.3 Visualisation of the physical interactions between ECs and PCs

To investigate the role of PCs in the EC–PC co-culture angiogenesis model, we visualised interactions between ECs and PCs by immunostaining. Architectural features of the parent vessel and the sprouts in EC–PC vessels were captured using CLSM, as shown in Fig. 3. ECs were stained for CD31, which is a specific

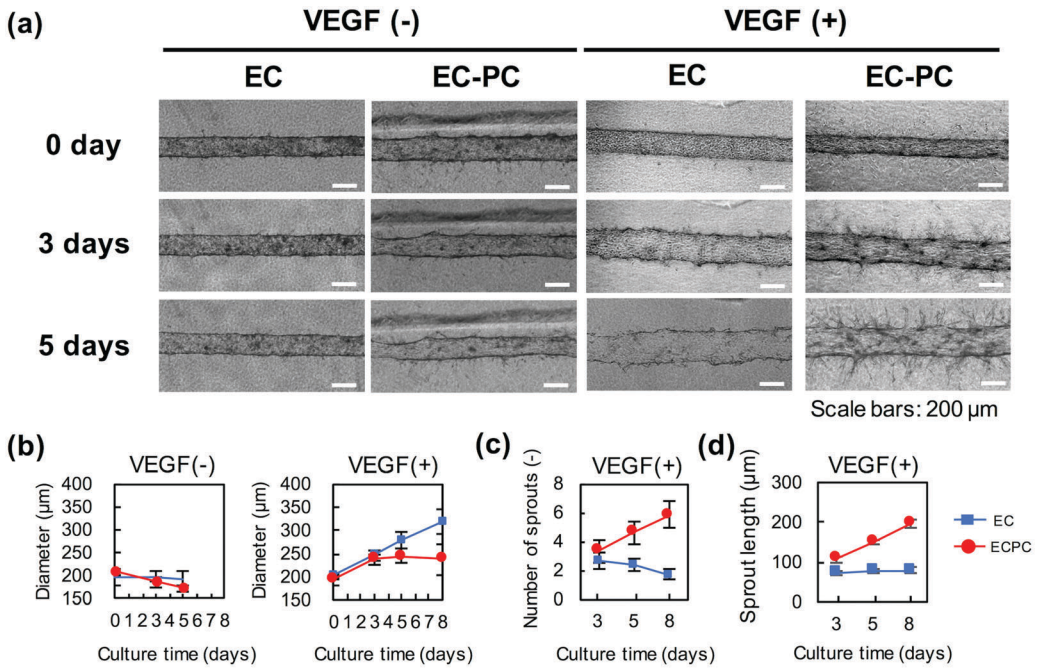

Fig. 2 EC mono-culture and EC–PC co-culture vessels cultured with or without additional VEGF. (a) Bright-field microscopy (BFM) images of EC mono-culture and EC–PC co-culture vessels when cultured with or without additional VEGF. The lines appearing above the EC–PC co-culture microvessels are reflections of the chamber under the microscope. [VEGF] = 50 ng mL^{-1}. (b) Diameter changes in the parent vessel over time in EC mono-culture and EC–PC co-culture vessels when cultured with or without additional VEGF. [VEGF] = 50 ng mL^{-1}. EC mono-culture: VEGF(−), n = 3; VEGF(+), $n \geqq 6$. EC–PC co-culture: VEGF(−), n = 5, VEGF(+), $n \geqq 3$. (c and d) Changes in the number of sprouts per 1 mm parent vessel (c) and the sprout length (d) over time in EC mono-culture and EC–PC co-culture vessels in the presence of additional VEGF. [VEGF] = 50 ng mL^{-1}. For sprout number, "n" represents the number of microvessels and EC mono-culture: $n \geqq 6$, EC–PC co-culture: $n \geqq 5$. For the sprout length, "n" represents the number of sprouts, and EC mono-culture: $n \geqq 31$, EC–PC co-culture: $n \geqq 50$.

marker for EC, whereas ECs and PCs together were stained for F-actin; this made the fluorescence signals overlap only in ECs, leaving PCs with signals from F-actin alone. Fig. 3b represents the whole EC–PC co-culture vessel observed after 5 days of culture with additional VEGF. Long and sharp spikes emerging from the parent vessel in the top image represented newly formed vessels as seen in BFM images, and the image below shows hair-like structures surrounding both the parent vessel and the sprouts, some of which are PCs. Taking a closer look at the parent vessel, ECs stained with CD31 were aligned in the horizontal direction, which does not usually occur in EC mono-culture vessels, and the cross-sectional image showed that the PC layer was separated from but covering the EC layer from the collagen side (Fig. 3c). In addition, as shown in Fig. 3d, time-dependent responses of ECs and PCs were captured, such that ECs and PCs were randomly distributed in the vessel wall at 0 day, but PCs formed a completely separated layer attached to the EC layer after 5 days. This separation of the PC layer from the EC layer and localisation of the PC layer in-between the EC layer and the collagen was also confirmed by 2-dimensional (2D) culture of the EC and PC mixture (Fig. S2, ESI†). In the 2D culture experiment, ECs and PCs were mixed at a 5 : 1 ratio, seeded onto the glass-bottomed dish covered with collagen, and cultured with EGM-2 containing additional VEGF for 5 days after the 2 day pre-culture period, following the same regimen as in 3D. Although ECs and PCs were randomly seeded onto the collagen at 0 day, ECs formed a layer on their own with a separate PC layer attached to it from the collagen side.

With regard to the sprout architecture, sprouts that appeared 2 days after VEGF addition were surrounded by hair-like PCs, with some PCs adhering to the sprout wall, possibly making the sprout slim and long, as seen in Fig. 3e. In addition, magnified images of the sprout obtained after 5 days of culture with additional VEGF clearly showed attachment of the PCs to the sprout wall from the collagen side stabilising the sprouts, as shown in Fig. 3f.

We visualised ECs and PCs and distinguished them from each other by immunostaining. These observations implied that the enhanced development of the sprouts and prevention of the parent vessel expansion by incorporation of the PCs resulted from PC attachment to the EC layer from the collagen side, providing mechanical support.

3.4 Quantitative analysis of angiogenic sprout characteristics using the OCT system

To assess angiogenesis in this microvessel model quantitatively, parameters such as sprout number, sprout length and sprout branch number were evaluated using an OCT system, which allows rapid 3D imaging without fluorescent labelling. In addition, based on these measurements, length and branch number can be deduced by simple image processing using ImageJ; the approximate diameter of the sprouts, which is

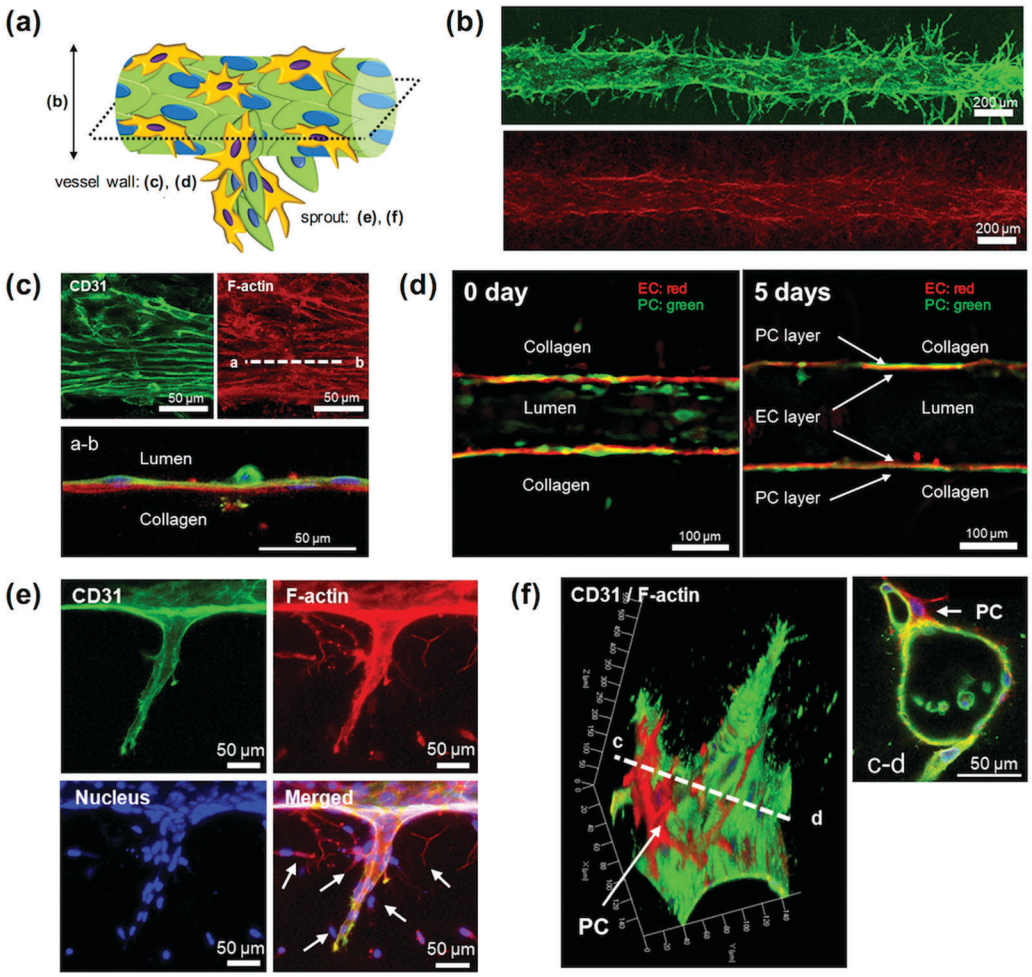

Fig. 3 Visualisation of the interactions between ECs and PCs in EC–PC co-culture vessels in VEGF-induced angiogenesis. (a) Schematic view of the EC–PC co-culture microvessel. (b) The whole vessel image obtained after 5 days of culture with additional VEGF. CD31-stained EC layer (green) is presented at the top, whereas F-actin of both ECs and PCs (red) is shown at the bottom. (c) Close-up image of the parent vessel wall and a cross-sectional image cut in the horizontal direction obtained after 5 days of culture with additional VEGF. The PC layer (red alone) was located at the basal side and separated from the EC layer (green and red). (d) Parent vessel images obtained after 0 day (left) and 5 days (right) of culture with additional VEGF. Some PCs (green: GFP) were located on the lumen side at 0 day, but PCs separated from the EC layer (red: CD31) completely at 5 days, attaching to the EC layer from the collagen side. (e) Image of sprouts obtained 2 days after culturing with additional VEGF. Hair-like PC cells (red alone, shown by arrows) surrounding the sprouts and some attaching to the sprouts. ECs are represented by CD31 in green and F-actin stained in red for both ECs and PCs. (f) 3D image of sprouts obtained after 5 days of culture with additional VEGF showing attachment of the PCs to the sprout wall. ECs are represented by CD31 in green and F-actin is stained in red for both ECs and PCs.

difficult to measure by other means, can also be estimated. Unlike the previous study in which we observed dynamic changes in the parent vessel and sprouts over time, in this study, we focused on characterising the details of the sprouts at specific time points using the OCT system.

Fig. 4a shows cross and side views of EC mono-culture and EC–PC co-culture vessels that were cultured for 5 days with additional VEGF in 3D reconstructed images (also Movies S1 and S2, ESI†). These 5 day vessels were subjected to evaluation using the OCT system. From these images, 3D morphological characteristics of the sprouts could be clearly seen, such that the sprouts were longer with a sharp tip in the EC–PC co-culture vessel, whereas those in the EC mono-culture vessel were short with a finger-like structure. Moreover, EC–PC co-culture vessels presented a greater number of branches, which was not usually observed in EC mono-culture vessels cultured under the same conditions. The number of sprouts in each microvessel can be obtained by numbering the extracted sprouts as shown in Fig. 4b, and the number of sprouts per 1 mm length of the parent vessel was 14.3 in an EC mono-culture vessel and 36.0 in an EC–PC co-culture vessel. These numbers were larger than those obtained from 2D CLSM images as shown in Fig. 2c, namely, 2.4 in EC mono-culture and 14.3 in EC–PC co-culture vessels. These differences arise from the fact that OCT takes into account sprouts in all directions in 3D, whereas 2D CLSM images capture only those in the same plane and the captured sprouts may actually be segments of the whole sprouts. In addition, the number of branches in each sprout can be derived from the extracted sprout image by binarisation and skeletonisation as shown in Fig. 4c. The length of each branch can also be

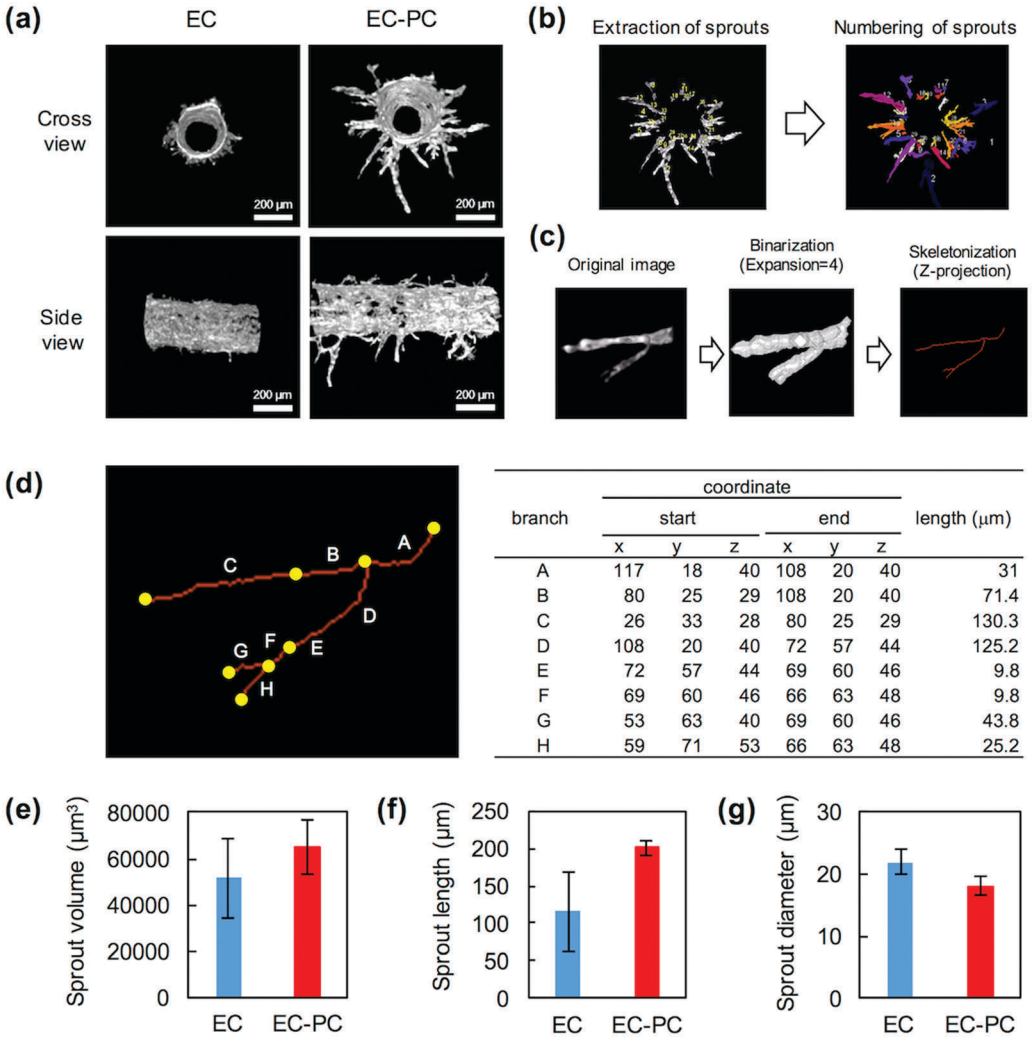

branch	coordinate						length (μm)
	start			end			
	x	y	z	x	y	z	
A	117	18	40	108	20	40	31
B	80	25	29	108	20	40	71.4
C	26	33	28	80	25	29	130.3
D	108	20	40	72	57	44	125.2
E	72	57	44	69	60	46	9.8
F	69	60	46	66	63	48	9.8
G	53	63	40	69	60	46	43.8
H	59	71	53	66	63	48	25.2

Fig. 4 Quantitative image analysis of sprout characteristics using the OCT system. (a) 3D cross and side views of representative EC mono-culture and EC–PC co-culture vessels that were cultured for 5 days with additional VEGF reconstructed from OCT cross-sectional images. (b) Extraction and numbering of sprouts from the original 3D EC–PC co-culture vessel image. (c) Image processing steps of binarisation and skeletonisation from the original sprout image for quantitative analysis. (d) Number of branches and length can be quantified by 3D co-ordinates (*x*, *y*, *z*) in the skeletonised image. (e–g) Average volume (e), length (f) and diameter (g) of the sprouts in the EC mono-culture (n = 10 spouts) or the EC–PC co-culture vessel (n = 36 sprouts).

obtained from the co-ordinates of the start point and the end point of each branch in the skeletonised images (Fig. 4d).

The results from analysing the sprout characteristics including average sprout volume, length and diameter in EC mono-culture and EC–PC co-culture vessels are shown in Fig. 4e–g. As shown in Fig. 4e, there was no huge difference in the average sprout volume, which was 51,645.6 ± 17,406.9 μm^3 in EC mono-culture and 65,076.2 ± 11,851.4 μm^3 in EC–PC co-culture vessels. Meanwhile, as already confirmed in Fig. 2d, the average sprout length was also greater in EC–PC co-culture (200.5 ± 10.1 μm) than in EC mono-culture (116.2 ± 52.8 μm) as shown in Fig. 4f, indicating that the sprout structure was tighter in EC–PC co-culture vessels. This was also confirmed by the data on the sprout diameter, which was slightly smaller in EC–PC co-culture (18.1 ± 1.4 μm) than in EC mono-culture (21.9 ± 2.0 μm), although the difference was not considerable.

These results showed that the OCT imaging system not only provides detailed 3D images of microvessels but also allows a quantitative analysis of sprout characteristics, including the numbers of branches of the sprouts.

4 Discussion

4.1 PCs prevent parent vessel expansion and enhance sprout formation and elongation by covering the EC layer

Angiogenesis is a multistep process which involves cell migration towards an angiogenic stimulus, sprout elongation and stabilization. Recently established *in vitro* systems to study EC–PC interactions in angiogenesis include a micropillar device,[15] which allows the observation of sprouting in a controlled manner; a tube formation assay,[22] which performs the reorganisation step

of angiogenesis; and a bead assay,[24] which displays the sprouting process in 3D. These tools shed light on the behaviour of PCs in angiogenic sprouting. However, these systems are only focused on the sprout extension and none succeeded to exhibit from the emergence of sprouts in the parent vessel wall to maturation of the newly formed vessel. Hence, the role of PCs in a more natural angiogenic setting remained unclear. To overcome this issue, we utilised a 3D microvessel model previously,[26,27] which enables angiogenesis to be captured from the appearance of sprouts in the parent vessel, since the parent vessel is equipped from the start by employing tissue engineering to establish an EC–PC co-culture system.

Interestingly, although ECs and PCs were randomly mixed together and seeded to construct a microvessel, only PCs migrated into the collagen and spontaneously formed a separate layer covering the EC layer after additional VEGF stimulation. PC migration was observed without additional VEGF, but migration was more intense with additional VEGF, and in 5 days PCs were completely separated from the ECs. This finding of PC migration prior to sprouting may support previous reports describing that PCs migrate first and secrete growth factors such as VEGF to lead to sprout formation.[30,31]

By applying the mixing method to construct microvessels, this 3D microvessel model can be adapted to mimic tissue with a high EC : PC ratio, such as skeletal muscles (10 : 1), since we know that EC–PC co-culture vessels can be stabilized with a ratio ranging from 5 : 1 to 10 : 1, raising the possibility of their use as a drug testing model for a broader range of applications. Nevertheless, our model is not suitable for modelling neural tissue as the percentage of PCs incorporated is too high, with an EC : PC ratio of 1 : 1, which makes the microvessel decompose in our model.[33] Adjusting the PC coverage not only permits the re-creation of microvessels from different parts of the body but also enables the control of vessel wall rigidity and sensitivity to chemotherapeutic drugs targeting the blood vessels. Furthermore, this EC–PC co-culture system could be a useful model for cancer treatment as the co-targeting of ECs and PCs may be a good strategy to combat tumour growth.[34]

From Fig. 2, during the 8 day culture with additional VEGF, incorporation of PCs prevented expansion of the parent vessel, which usually occurs in EC mono-culture in response to VEGF stimulation, and led to increases in the number and length of sprouts compared with those in the EC mono-culture. It would be interesting to study the effect of PCs in the longer term on the stability of the parent vessel and the sprouts.

Moreover, OCT analysis clearly indicated that the formed sprouts had a long pencil-like structure with a sharp tip, whereas those in the EC mono-culture had a finger-like structure with a round head, as seen in Fig. 4a. Furthermore, the analysis of the OCT images in Fig. 4e and f revealed that the formed sprouts were not only longer but also tighter in EC–PC co-culture vessels, which was difficult to conclude from CLSM images. The underlying mechanism for this tightening of the parent vessel and sprouts in the EC–PC co-culture vessel could involve the PCs adhering to the parent vessel and the sprouts from the collagen side providing mechanical support, as observed in the close-up images of the parent vessel and the sprouts (Fig. 3), and as also seen in the previous report.[15] Another notable feature of EC–PC co-culture vessels is the alignment of the ECs in the parent vessel in the horizontal direction, which was never seen in EC mono-culture vessels. We assume that this alignment could also result from the mechanical forces applied to ECs by PCs, as it has been previously reported that EC alignment can occur perpendicular to the direction of stretching, which may be caused by PC contraction or movements.[35]

Although in our study we observed PCs enhancing sprout elongation and formation in response to VEGF stimulation most of the time, we also observed PCs preventing sprout formation in rare cases with no prior PC migration into the collagen, despite VEGF stimulation, the cause of which was unclear. Since PCs are considered to have opposite roles in the context of angiogenesis, suppressing or promoting EC growth depending on the circumstances, it would be worthwhile to focus on EC–PC interactions under specific conditions using our microvessel model. Moreover, EC and PC interactions not only include physical association but also paracrine signalling, and our model can be a useful tool to study how paracrine factors from the PCs affect EC behaviour. This may be done by culturing EC mono-culture vessels in PC conditioned media. Furthermore, since the microvessels possess open ends to which tubes can be connected to apply a flow, perfusion can also be tested.

4.2 3D visualisation using OCT achieved quantitative analysis of sprout characteristics

Previously, Del Amo's group succeeded in quantifying the number and length of angiogenic sprouts in 3D in a microfluidic platform containing one central chamber to which collagen was added and two lateral channels containing media with growth factors separated by micropillars.[36] In this platform, sprouts were formed between two micropillars and the 3D structure was reconstructed by computationally processing 2D images of the sprouting region and stacking them. However, there were limitations to this system in terms of recreating the physiological environment, such that this microfluidic platform only allowed reconstruction of the sprout region in 3D, since this model does not contain the parent vessel region. In addition, only the length of sprouts was focused on and information on the volume and diameter was not gathered, although these can be useful parameters. Moreover, previous methods required immunostaining to obtain information on 3D distribution prior to observation with CLSM.[15] In our study, by combining OCT analysis, we not only captured the 3D structure of each sprout emerging from the pre-existing parent vessel but also succeeded in quantitatively assessing characteristics such as diameter and volume, as shown in Fig. 4. The sprout lengths deduced from the 3D OCT images should be more precise than those obtained from the 2D CLSM images of the microvessels cut in half across the center since 2D images only show the sprouts in the same plane and extension angles are not taken into account. (Fig. 2d) Being able to gather

information on these parameters will be useful for testing the effects of drugs.

Using OCT imaging and analysis, the following was achieved: (i) identification of the locations of the components in 3D, (ii) distinguishing the sprouts from the parent vessel and (iii) quantifying sprout characteristics such as number, volume and length, as shown in Fig. 4e–g. Moreover, in this study, we also achieved a quantitative analysis of the sprout diameter and the branch number, which was previously difficult, of the OCT system for the first time.

5 Conclusion

We developed a 3D *in vitro* EC–PC co-culture microvessel model, which enables observation of how the presence of PCs affects not only the sprouting region but also the parent vessel in angiogenesis. The incorporation of PCs led to reduced parent vessel expansion and enhanced sprout formation in response to VEGF stimulation, which is favourable for assessing angiogenesis. By combining with OCT analysis, sprout characteristics such as volume, length and diameter can be obtained, which can be useful for drug testing.

Conflicts of interest

Dr Masayoshi Kobayashi and Mr Keisuke Kato are employees of SCREEN Holdings Co. Ltd.

Acknowledgements

This work was partly supported by JSPS KAKENHI Grant Numbers JP 17H04170 and JP 17K19368. The authors thank Mr Yasuhiro Ookawa and Dr Koji Fujimoto (Dai Nippon Printing Co., Ltd) for their assistance in the PDMS device fabrication, Dr Yosuke Hiraoka (Nitta Gelatin Inc.) for his kind support in collagen preparation, Mr Kenji Ueyama (SCREEN Holdings Co., Ltd) for his advice regarding OCT and Ms Eri Otsuka (The University of Tokyo) for her technical assistance.

References

1 H. Gerhardt, *Organogenesis*, 2008, **4**, 241–246.
2 G. Bergers and S. Song, *Neuro-Oncology*, 2005, **7**, 452–464.
3 H. Gerhardt and C. Betsholtz, *Cell Tissue Res.*, 2003, **314**, 15–23.
4 S. Wong, J. Rowley, A. Redpath, J. Tilman, T. Fellous and J. Johnson, *Pharmacol. Ther.*, 2015, **151**, 107–120.
5 A. Geevarghese and I. Herman, *Transl. Res.*, 2014, **163**, 296–306.
6 P. Stapor, R. Sweat, D. Dashti, A. Betancourt and W. Murfee, *J. Vasc. Res.*, 2014, **51**, 163–174.
7 A. Armulik, A. Abramsson and C. Betsholtz, *Circ. Res.*, 2005, **97**, 512–523.
8 C. Suri, P. Jones, S. Patan, S. Bartunkova, P. Maisonpierre, S. Davis, T. Sato and G. Yancopoulos, *Cell*, 1996, **87**, 1171–1180.
9 G. Thurston, C. Suri, K. Smith, J. McClain, T. N. Sato, G. D. Yancopoulos and D. M. McDonald, *Science*, 1999, **286**, 2511–2514.
10 N. Akhtar, E. B. Dickerson and R. Auerbach, *Angiogenesis*, 2002, **5**, 75–80.
11 Z. Tahergorabi and M. Khazaei, *Iran. J. Basic Med. Sci.*, 2011, **15**, 1110–1126.
12 M. S. Rogers, A. E. Birsner and R. J. D'Amato, *Nat. Protoc.*, 2007, **2**, 2545–2550.
13 W. AlMalki, I. Shahid, A. Mehdi and M. Hafeez, *Indian J. Pharmacol.*, 2014, **46**, 251–256.
14 J. Xu, T. Gong, B. C. Heng and C. F. Zhang, *FASEB J.*, 2017, **31**, 1775–1786.
15 J. Kim, M. Chung, S. Kim, D. Jo, J. Kim and N. Jeon, *PLoS One*, 2015, 10.
16 Y. Kim, Y. Takahashi, N. Kato and Y. Matsunaga, *J. Mater. Chem. B*, 2015, **3**, 8154–8161.
17 Y. Kim, M. Tachibana, M. Umezu and Y. Matsunaga, *J. Mater. Chem. B*, 2016, **4**, 1740–1746.
18 Y. Kim and Y. Matsunaga, *J. Mater. Chem. B*, 2017, **5**, 4307–4321.
19 Y. Matsunaga, Y. Morimoto and S. Takeuchi, *Adv. Mater.*, 2011, **23**, H90–H94.
20 H. Onoe, T. Okitsu, A. Itou, M. Kato-Negishi, R. Gojo, D. Kiriya, K. Sato, S. Miura, S. Iwanaga, K. Kuribayashi-Shigetomi, Y. Matsunaga, Y. Shimoyama and S. Takeuchi, *Nat. Mater.*, 2013, **12**, 584–590.
21 A. Goodwin, *Microvasc. Res.*, 2007, **74**, 172–183.
22 Z. Zhou, F. Pausch, U. Schlotzer-Schrehardt, B. Brachvogel and E. Poschl, *Histochem. Cell Biol.*, 2016, **145**, 511–525.
23 J. Waters, M. Kluger, M. Graham, W. Chang, J. Bradley and J. Pober, *J. Vasc. Res.*, 2013, **50**, 324–331.
24 J. Eglinger, H. Karsjens and E. Lammert, *Inflammation Regener.*, 2017, **37**, 2.
25 I. Tattersall, J. Du, Z. Cong, B. Cho, A. Klein, C. Dieck, R. Chaudhri, H. Cuervo, J. Herts and J. Kitajewski, *Angiogenesis*, 2016, **19**, 201–215.
26 H. Takahashi, K. Kato, K. Ueyama, M. Kobayashi, G. Baik, Y. Yukawa, J. Suehiro and Y. Matsunaga, *Sci. Rep.*, 2017, 7.
27 J. Pauty, R. Usuba, H. Takahashi, J. Suehiro, K. Fujisawa, K. Yano, T. Nishizawa and Y. T. Matsunaga, *Nanotheranostics*, 2017, **1**, 103–113.
28 M. Kabara, J. Kawabe, M. Matsuki, Y. Hira, A. Minoshima, K. Shimamura, A. Yamauchi, T. Aonuma, M. Nishimura, Y. Saito, N. Takehara and N. Hasebe, *Lab. Invest.*, 2014, **94**, 1340–1354.
29 J. Pauty, R. Usuba, I. G. Cheng, L. Hespel, H. Takahashi, K. Kato, M. Kobayashi, H. Nakajima, E. Lee, F. Yger, F. Soncin and Y. T. Matsunaga, *EBioMedicine*, 2018, **27**, 225–236.
30 U. Ozerdem and W. B. Stallcup, *Angiogenesis*, 2003, **6**, 241–249.
31 U. Ozerdem and W. B. Stallcup, *Angiogenesis*, 2004, **7**, 269–276.
32 M. Heiss, M. Hellström, M. Kalén, T. May, H. Weber, M. Hecker, H. G. Augustin and T. Korff, *FASEB J.*, 2015, **29**, 3076–3084.
33 D. Shepro and N. Morel, *FASEB J.*, 1993, **7**, 1031–1038.
34 E. Kang and J. W. Shin, *Int. J. Nanomed.*, 2016, **11**, 2397–2406.
35 J. Wang, P. Goldschmidt-Clermont, J. Wille and F. Yin, *J. Biomech.*, 2001, **34**, 1563–1572.
36 C. Del Amo, C. Borau, R. Gutiérrez, J. Asín and J. M. García-Aznar, *J. Biomech.*, 2016, **49**, 1340–1346.

